PAPER

CrossMark
click for updates

Synthesis, characterization, photophysics, and anion binding properties of platinum(II) acetylide complexes with urea group†

Zhi-Hui Zhang, Jiewei Liu, Li-Qi Wan, Fang-Ru Jiang, Chi-Keung Lam, Bao-Hui Ye, Zhengping Qiao and Hsiu-Yi Chao*

A new class of platinum(II) acetylide complexes with urea group, [Pt(tBu₃tpy)(C≡CC₆H₄-4-NHC(O)-NHC₆H₄-4-R)](OTf) (tBu₃tpy = 4,4′,4″-tri-*tert*-butyl-2,2′:6′,2″-terpyridine; R = H (**3a**), Cl (**3b**), CF₃ (**3c**), and NO₂ (**3d**)), has been synthesized and characterized. The crystal structures of **3a**, **3a·DMF·THF**, **3b·CH₃CN**, and **3c·CH₃CN** have been determined by X-ray diffraction. Upon excitation at λ > 380 nm, the solid samples of complexes **3a–3d** show orange light at 298 K. The anion binding properties of complexes **3a–3d** have been studied by UV-vis titration experiments in CH₃CN and DMSO. In general, the log *K* values of **3a–3d** with the same anion in CH₃CN depend on the substituent R on the acetylide ligand of **3a–3d** and follow this order: R = NO₂ (**3d**) > CF₃ (**3c**) > Cl (**3b**) > H (**3a**). For the same complex with different anions, the log *K* values are in the following order: F⁻ > OAc⁻ > Cl⁻ > Br⁻ ≈ HSO₄⁻ ≈ NO₃⁻ > I⁻, which is in accordance with the decrease in the basicity of anions. Complex **3d** with NO₂ group shows a dramatic colour change towards F⁻ in DMSO, allowing the naked eye detection of F⁻.

Introduction

Anion sensors have attracted increasing interest over the past decade because of the crucial importance of anions and their potential applications in chemistry, biology as well as the environment.[1] Since the pioneering work of Park and Simmons on the first anion sensor,[2] a variety of artificial anion receptors have been designed and synthesized for the stimulation of host–guest interactions within the supramolecular chemistry. Thus, considerable effort has been devoted to the exploitation of selective anion sensors. An ideal anion sensor consists of a receptor center for binding anions, which is covalently linked to a reporting center for the signaling of interactions.[3] A sensing signal is generated once the receptor center binds anions through non-covalent interactions, and the binding of such species could produce changes in the photophysical and redox properties of the reporter unit. Urea,[4,5] thiourea,[5] amide,[6] and guanidinium[7] based organic

compounds have been reported as anion sensors due to their specific hydrogen bonding interactions towards anions. Among them, urea-based receptors have been extensively studied owing to their unique geometry (two hydrogen bonds towards anions) and their easy modification through organic synthesis.[4]

While the early studies mainly focused on the organic anion sensors,[8] metal complexes based anion sensors have also received immense attention. Metal complexes could have some intrinsic properties, such as redox and luminescence, and the metal center can directly interact with anions. Thus, anion recognition and sensing by metal complexes are supposed to extend the detection of anion binding. Iron(II),[9] rhenium(I),[10] ruthenium(II),[11] iridium,[12] gold(I),[13] terbium(III),[14] and gold(I)–copper(I)[15] complexes with urea group have been reported as anion sensors. Amongst various metal complexes, a great deal of attention has been particularly given to the platinum(II) acetylide complexes because of their rich photoluminescence properties.[16] The square planar geometry of platinum(II) also allows the Pt···Pt interactions, which could affect the properties of electronic excited states. In this regard, platinum(II) acetylide complexes have been used as sensors for VOC,[17] pH,[18] ions,[19] temperature,[18a,20] and mechanical force.[17c,21] In addition, the charge transfer absorption in the visible region with the corresponding higher quantum yield photoluminescence of platinum(II) acetylide complexes also facilitates applications such as molecular recognition,[22] photo-

MOE Key Laboratory of Bioinorganic and Synthetic Chemistry, School of Chemistry and Chemical Engineering, Sun Yat-Sen University, Guangzhou 510275, China. E-mail: zhaoxy@mail.sysu.edu.cn; Fax: (+86)020-84112245; Tel: (+86)020-84110062
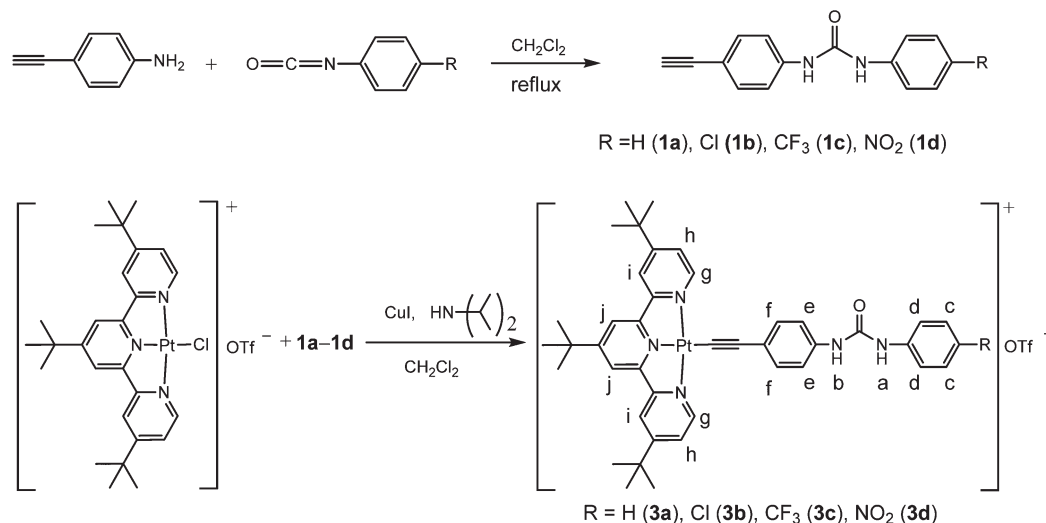
Scheme 1 Synthetic route of platinum(II) acetylide complexes **3a–3d**.

catalysts,[23] energy conversion materials,[24] electroluminescence[25] as well as broadband nonlinear transmission materials.[26] However, to the best of our knowledge, the study of anion-sensing properties of platinum(II) acetylide complexes has been less explored.[27]

Our group has a long-term interest in the study of the relationship between the structures and anion-binding properties of metal complexes.[13a,13b] To extend our study, in this research, we have synthesized a series of platinum(II) acetylide complexes with urea group [Pt(^{t}Bu$_3$tpy)(C≡CC$_6$H$_4$-4-NHC(O)-NHC$_6$H$_5$-R)](OTf) (^{t}Bu$_3$tpy = 4,4′,4″-tri-*tert*-butyl-2,2′:6′,2″-terpyridine; R = H (**3a**), Cl (**3b**), CF$_3$ (**3c**), NO$_2$ (**3d**); Scheme 1). Their photophysical and anion-binding properties have been investigated. We envisaged that if the photophysical properties of these platinum(II) acetylide complexes could be changed when they interact with anions through hydrogen bonds between the urea N–H(s) of the complexes and anions, they could be used as anion sensors. In addition, the effect of the substituent R of the acetylide ligand on the anion-binding ability of the complexes **3a–3d** has also been examined. Interestingly, complex **3d** showed a significant colour change when it interacted towards F$^-$ in DMSO, allowing the naked eye detection of F$^-$.

Results and discussion

Synthesis and characterization

Scheme 1 shows the synthetic routes of the acetylide ligands (**1a–1d**) and platinum(II) acetylide complexes (**3a–3d**). The acetylide ligands, HC≡CC$_6$H$_4$-4-NHC(O)NHC$_6$H$_4$-4-R (R = H (**1a**), Cl (**1b**), CF$_3$ (**1c**), NO$_2$(**1d**)), were prepared by the reaction of 4-ethynylaniline with the corresponding isocyanate in a molar ratio of 1 : 1 in refluxing dichloromethane. Furthermore, the reactions of [Pt(^{t}Bu$_3$tpy)Cl](OTf) (**2**) (^{t}Bu$_3$tpy = 4,4′,4″-tri-*tert*-

butyl-2,2′:6′,2″-terpyridine) with **1a–1d** in the presence of CuI and diisopropylamine in dichloromethane gave **3a–3d**, respectively. All the platinum(II) acetylide complexes **3a–3d** were characterized by ^{1}H NMR, IR as well as ESI-MS and gave satisfactory elemental analyses. They are air-stable in the solid state at 298 K.

In the ^{1}H NMR spectra of the platinum(II) acetylide complexes **3a–3d** in DMSO-d_6, the protons of N–H on the acetylide ligands of the complexes show resonance at *ca.* 8.65–9.46 ppm. The chemical shifts are in the following order: **3a** < **3b** < **3c** < **3d**, which is in accordance with the increasing electron-withdrawing ability of the substituent R on the acetylide ligand. In addition, the chemical shifts at *ca.* 6.96–8.18 ppm are attributed to the resonance of the protons on the aromatic rings of the acetylide ligand. The chemical shifts at *ca.* 7.85–9.02 ppm as well as 1.43 and 1.53 ppm are attributed to the resonance of the protons on the ^{t}Bu$_3$tpy ligand. The IR spectra of **3a–3d** reveal the bands at 3350–3433 and 1610–1641 cm^{-1}, which are the characteristic of ν(N–H) and ν(C=O) of the acetylide ligands, respectively.

Crystal structures of 3a, 3a·DMF·THF, 3b·CH$_3$CN, and 3c·CH$_3$CN

The crystal structures of the platinum(II) acetylide complexes **3a**, **3a·DMF·THF**, **3b·CH$_3$CN**, and **3c·CH$_3$CN** have been determined by X-ray diffraction. Their crystallographic data as well as selected bond distances and angles are listed in Table S1 (ESI†) and Table 1. Fig. 1 shows the perspective view of **3a** (for **3a·DMF·THF**, **3b·CH$_3$CN**, and **3c·CH$_3$CN**, see Fig. S1–S3 (ESI†)). The platinum(II) coordination geometry in these complexes is distorted square-planar. The Pt–N bond distances are in the range of 1.949(5)–2.029(5) Å, which are similar to those of other related platinum(II) acetylide complexes.[22c,27d,28] The Pt1–C1 and C1≡C2 bond distances are in the range of 1.966(8)–1.992(8) and 1.206(10)–1.219(10) Å, respectively,

Table 1 Selected bond distances (Å) and bond angles (°) of complexes **3a**, **3a·DMF·THF**, **3b·CH₃CN**, and **3c·CH₃CN**

	3a	3a·DMF·THF	3b·CH₃CN	3c·CH₃CN
Pt⋯Pt (shortest)	5.804	9.253	4.931	5.139
Pt1–N1	2.027(6)	2.020(4)	2.029(5)	2.027(3)
Pt1–N2	1.956(6)	1.949(5)	1.973(6)	1.960(3)
Pt1–N3	2.026(6)	2.015(4)	2.022(5)	2.017(3)
Pt1–C1	1.967(7)	1.966(8)	1.992(8)	1.971(5)
C1–C2	1.219(10)	1.213(10)	1.206(10)	1.210(7)
C36–O1	1.154(13)	1.219(8)	1.225(7)	1.208(6)
N1–Pt1–N2	80.2(2)	80.08(17)	80.39(19)	80.41(13)
N2–Pt1–N3	80.6(2)	80.66(17)	80.41(17)	80.46(13)
N1–Pt1–N3	160.7(2)	160.63(18)	160.79(19)	160.87(13)
N1–Pt1–C1	100.6(3)	99.2(2)	98.6(2)	98.82(15)
N2–Pt1–C1	178.4(3)	179.6(2)	179.0(2)	179.12(16)
N3–Pt1–C1	98.6(3)	99.4(2)	100.6(2)	100.32(15)
Pt1–C1–C2	176.0(6)	177.3(7)	177.0(5)	176.8(4)
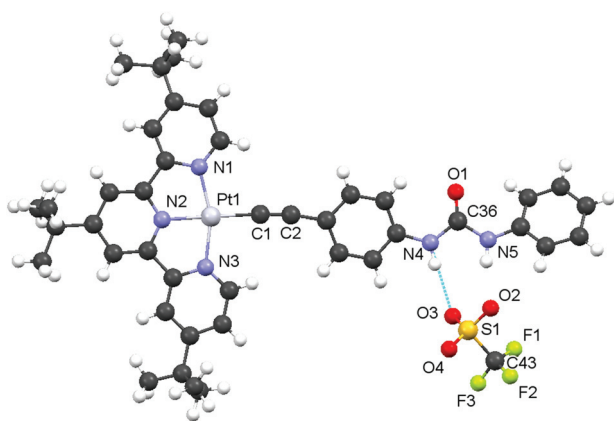
Fig. 1 Perspective view of **3a**.

which are comparable to those of other related platinum(II) acetylide complexes.[27d,28] The N1–Pt1–N2, N2–Pt1–N3, and N1–Pt1–N3 angles are *ca.* 80°, 80°, and 160°, respectively, which could be due to the geometric constraints of ᵗBu₃tpy ligand. Each pair of complex cations reveals a head-to-tail stacking with the shortest Pt⋯Pt distance of *ca.* 4.931–9.841 Å. In addition, there is a hydrogen bond interaction between the N–H of the urea group on the acetylide ligand and the oxygen atom of the triflate anion. The hydrogen bond parameters are listed in Table S2 (ESI†).

Fig. 2 shows the stacking patterns of adjacent planar platinum(II) moieties as well as the arrangement for complexes **3a**, **3a·DMF·THF**, **3b·CH₃CN**, and **3c·CH₃CN**. These platinum(II) acetylide complexes with different acetylide ligands tend to pack in diverse arrangements. Their adjacent platinum(II) moieties display an antiparallel stacking pattern. Fig. 2(a) shows the molecular packing of **3a**, in which the adjacent Pt atoms are in the zigzag arrangement with the Pt⋯Pt⋯Pt angle of 170.39° and the Pt⋯Pt distance alternating between 5.804 and 8.575 Å. In addition, no significant Pt⋯Pt or π⋯π interaction is observed from the crystal packing because of the bulky *tert*-

butyl groups on the terpyridyl ligands, which prevent the neighboring molecules from getting into close proximity with each other. While viewed along the *c* axis, the platinum atoms are almost superimposable to give a zigzag [Pt]ₙ chain. The individual molecules in the dimers are rotated with respect to their neighbors, with a C–Pt–P–C torsion angle of 180° and a partial stacking of the aromatic terpyridyl units. Unlike **3a**, in which the Pt metal center shows a strong propensity to form a zigzag chains with shorter intermolecular Pt⋯Pt contacts, the molecular packing in **3a·DMF·THF** exhibits a long distance between adjoining platinum atoms caused by the insertion of solvent molecules into the lattice, allowing two types of Pt⋯Pt distances to form a hexagon (Fig. 2(b)). The adjacent Pt⋯Pt distance is 9.253 Å between the platinum atoms arranged in the same order, while for those in the head-to-tail arrangement, the nearest Pt⋯Pt distance is 9.841 Å. The view along the *c* axis shows that the platinum atoms are arranged in a honeycomb lattice. THF molecules are inserted into the lattice through the three C–H⋯O hydrogen bonds (d(H⋯O1) = 2.667 Å, ∠(C–H⋯O1) = 171.25°; d(H⋯O2) = 2.528 Å, ∠(C–H⋯O2) = 173.36°; d(H⋯O3) = 2.618 Å, ∠(C–H⋯O3) = 153.56°), whereas DMF molecules form two C–H⋯O hydrogen bonds with two hydrogen atoms of pyridine ring (d(H⋯O1) = 2.458 Å, ∠(C–H⋯O1) = 156.73°, d(H⋯O2) = 2.588 Å, ∠(C–H⋯O2) = 162.30°). It is interesting to note that the stacking varies in **3a** with/without solvates. This difference may indicate that the aggregation of **3a** is solvate-dependent.

Fig. 2(c) shows the molecular packing of **3b·CH₃CN**, in which CH₃CN molecule is inserted into the lattice through the C–H⋯N interaction between the hydrogen atom on the pyridine ring and the nitrogen atom on the acetonitrile molecule (d(H⋯N) = 2.655 Å, ∠(C–H⋯N) = 128.50°). When viewed along the *a* axis, the adjacent Pt atoms form a head-to-tail dimeric structure with the adjacent Pt⋯Pt distance alternating between 4.931 and 10.001 Å, giving a zigzag [Pt]ₙ chain with a Pt–Pt–Pt angle of 159.16°. The shortest Pt⋯Pt distance is 4.931 Å, which is shorter than that of **3a**, while the distance between the Pt atoms of diverse adjacent dimeric unit is longer (10.001 Å). This could be due to the insertion of CH₃CN molecule into the cavity because of which the distance between neighboring dimeric units increases, while the Pt⋯Pt distance in the dimeric Pt atoms decreases. The stacking pattern of **3c·CH₃CN** has the same orientation as that of **3b·CH₃CN** (Fig. 2(d)). Both of them exist as sequential dimeric units with no evidence of Pt⋯Pt contacts. The shortest Pt⋯Pt distance of **3c·CH₃CN** is 5.139 Å, which is farther than that of **3b·CH₃CN** (4.931 Å). However, the distance between the Pt atoms of nearby dimers decreases to 9.968 Å. Moreover, the Pt–Pt–Pt angle of zigzag [Pt]ₙ chain is 158.31° when viewed from the *c* axis. Although the CH₃CN molecules are found in the crystal structure, there is no significant interaction between the solvent molecule (CH₃CN) and *tert*-butyl group. The crystal structures of **3b·CH₃CN** and **3c·CH₃CN** are other examples of solvent-dependent aggregation, which indicates that the molecules tend to pack in the same aggregation in the same solvent.
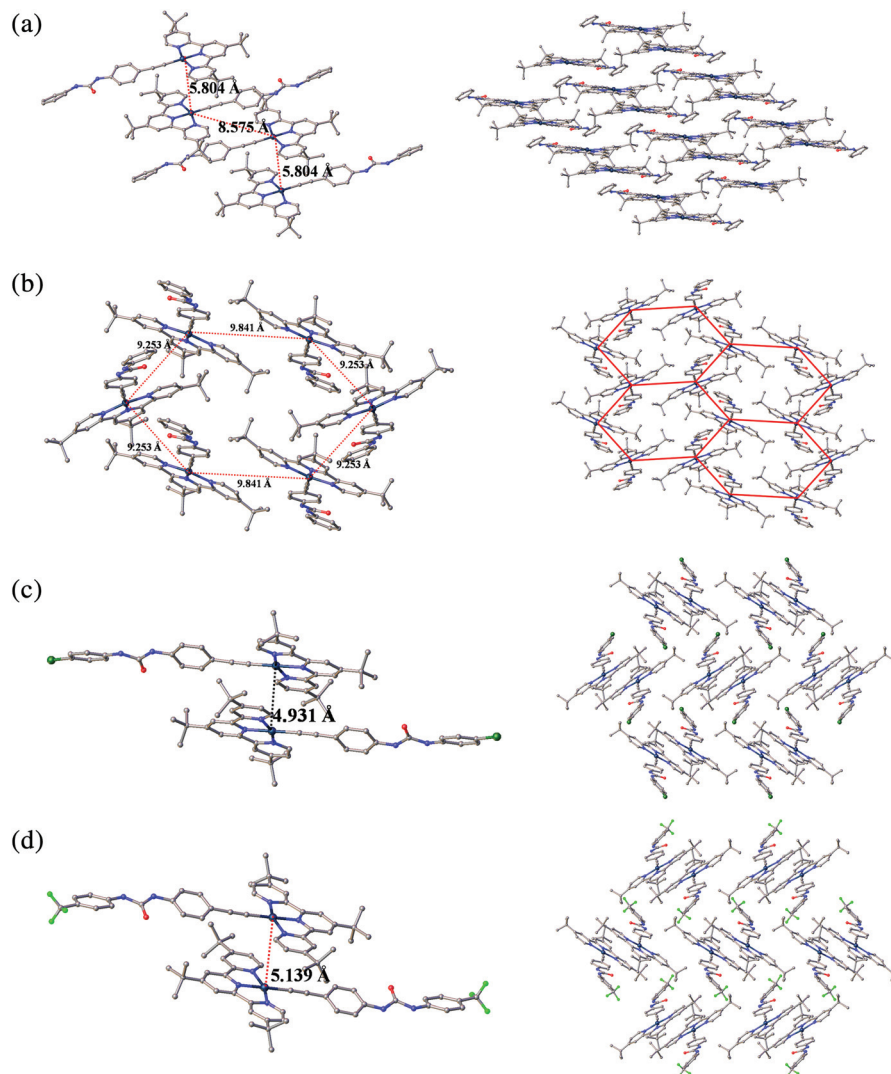
Fig. 2 Packing diagrams of (a) **3a**, (b) **3a·DMF·THF**, (c) **3b·CH₃CN**, and (d) **3c·CH₃CN** (left: stacking patterns of adjacent planar platinum(II) moieties; right: arrangement of the molecules; counter-anions are omitted for clarity).

Electronic absorption and emission spectra of complexes 3a–3d

The photophysical data for the acetylide ligands (**1a–1d**) and complexes (**3a–3d**) are summarized in Table S3 (ESI†) and Table 2, respectively. The electronic absorption spectra of **3a–3c** in acetonitrile show high-energy bands at 247–339 nm, which are assigned as the $\pi \rightarrow \pi^{\star}$ transitions of the $^{t}Bu_3$tpy and acetylide ligands (Fig. 3). For **3d** in acetonitrile, the electronic absorption bands at 312, 328, and 339 nm could be due to the charge transfer transition from the amide to the NO_2 group of the acetylide ligand.[13b] The low-energy bands of **3a–3d** in acetonitrile at 398–464 nm are ascribed to the admixture of MLCT ($d\pi(Pt) \rightarrow \pi^{\star}(^{t}Bu_3$tpy)) and LLCT ($\pi(C\equiv C$-$C_6H_4$-NH-C(O)-NH-$C_6H_4$-4-R) $\rightarrow \pi^{\star}(^{t}Bu_3$tpy)) transitions. The ground-state complex aggregation of **3a** in DMSO has also been studied. When the concentration of **3a** in DMSO increases from 1×10^{-5} to 1×10^{-3} mol dm^{-3}, the absorbance at 510 nm obeys

Beer's law (Fig. S4 and S5, ESI†), indicating that there is no aggregation of **3a** in DMSO in the concentration ranging from 10^{-5} to 10^{-3} mol dm^{-3}. This result may be due to the steric effect from the bulky $^{t}Bu_3$tpy ligand, preventing the aggregation of **3a**.[29]

It is interesting to note that platinum(II) acetylide complexes **3a–3d** exhibit different colours in different solvents. Because **3a** has the better solubility in solvents, it has been used to study the solvent effect on the electronic absorption spectrum. Fig. 4(a) shows the colours of **3a** at a concentration of 2.7×10^{-5} mol dm^{-3} in different solvents: light yellow (DMSO, CH₃CN, and CH₃OH), orange (CH₃C(O)CH₃), and pale red (CH₂Cl₂ and THF). Fig. 4(b) shows the electronic absorption spectra of **3a** in 370–700 nm in various solvents. The low-energy absorption maximum is in the order: CH₃OH (458 nm) < CH₃CN (464 nm) < DMSO (472 nm) < CH₃C(O)CH₃ (476 nm) < THF (492 nm) < CH₂Cl₂ (498 nm) depending on the solvent

Dalton Transactions

Paper

Table 2 Photophysical data of complexes **3a–3d** at 298 K

Complex	Medium	λ_{abs}/nm (ε/dm^3 mol^{-1} cm^{-1})	λ_{em}/nm[a] (τ_0/μs)
3a	DMSO	247 (sh, 43 150), 289 (61 480), 329 (sh, 16 180), 344 (14 300), 384 (sh, 4830), 407 (5290), 472 (7170)	
	CH$_3$CN	247 (54 280), 259 (sh, 51 280), 285 (80 320), 323 (sh, 21 320), 383 (sh, 5240), 405 (5820), 464 (6940)	
	THF	249 (41 440), 287 (64 960), 340 (sh, 14 740), 388 (sh, 4330), 412 (4880), 492 (5760)	
	CH$_2$Cl$_2$	231 (39 220), 251 (44 550), 287 (67 440), 338 (15 890), 411 (5330), 498 (5870)	
	CH$_3$C(O)CH$_3$	328 (15 960), 339 (16 150), 389 (sh, 5130), 409 (5870), 476 (7610)	
	CH$_3$OH	249 (45 070), 285 (73 670), 325 (sh, 18 630), 339 (17 520), 382 (sh, 4830), 409 (5500), 458 (5990)	
	Solid		616 (0.426)
3b	DMSO	260 (sh, 40 160), 290 (69 350), 329 (sh, 19 880), 344 (16 690), 404 (sh, 4430), 469 (5640)	
	CH$_3$CN	247 (39 105), 285 (68 455), 324 (sh, 17 720), 339 (15 530), 403 (sh, 4310), 460 (5160)	
	THF	289 (41 830), 340 (sh, 3440), 413 (2670), 493 (3020)	
	CH$_3$OH	286 (80 060), 326 (sh, 18 290), 339 (17 770), 395 (sh, 5350), 453 (6380)	
	CH$_2$Cl$_2$	287 (78 500), 339 (17 500), 412 (5240), 502 (5880)	
	Solid		607 (0.345)
3c	DMSO	260 (sh, 41 430), 291 (65 140), 332 (sh, 15 990), 344 (14 180), 404 (sh, 4080), 469 (5610)	
	CH$_3$CN	247 (43 850), 286 (72 810), 324 (sh, 17 950), 339 (16 670), 402 (sh, 4670), 459 (5700)	
	Solid		601 (0.249)
3d	DMSO	260 (sh, 42 520), 285 (51 520), 332 (sh, 30 800), 346 (34 320), 468 (7480)	
	CH$_3$CN	246 (39 105), 273 (sh, 65 760), 284 (45 850), 312 (28 780), 328 (32 720), 339 (35 280), 459 (4430)	
	Solid		599 (0.502)

[a] The emission of **3a–3d** was too weak to be observed in these solvents.
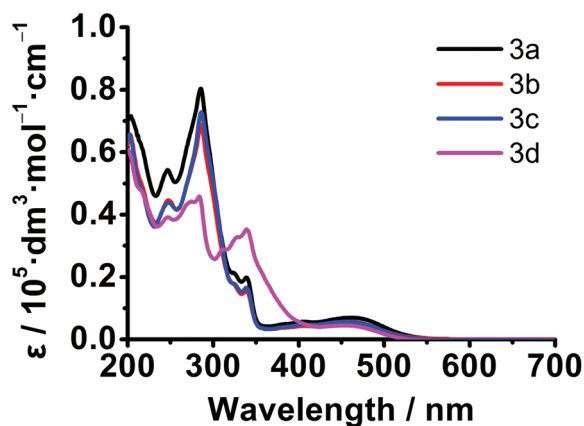
Fig. 3 Electronic absorption spectra of **3a–3d** in acetonitrile at 298 K.

polarity (Table S4, ESI†). However, there is no clear trend between the absorption maximum and solvent polarity. Similar trend can also been observed for **3b** (Table S4 and Fig. S6, ESI†). The solvent-dependent absorption bands indicate their charge-transfer character in nature.

The excitation of complexes **3a–3d** in the solid state at $\lambda >$ 380 nm produces orange light. The emission maxima of **3a–3d** in the solid state at 298 K are in the following order: 616 nm (**3a**) > 607 nm (**3b**) > 601 nm (**3c**) > 599 nm (**3d**), which is in accordance with the increasing electron-withdrawing ability of the substituent R on the acetylide ligand (R = H (**3a**) < Cl (**3b**) < CF$_3$ (**3c**) < NO$_2$ (**3d**)) (Fig. 5). The lifetime of these emission bands is 0.249–0.502 μs, indicating the nature of the triplet excited state. The stronger electron-withdrawing acetylide ligands could reduce the energy of dπ(Pt)- and π(acetylide ligand)-based HOMO.[26d] Thus, the emission band at 599–616 nm for **3a–3d** in the solid state is tentatively assigned

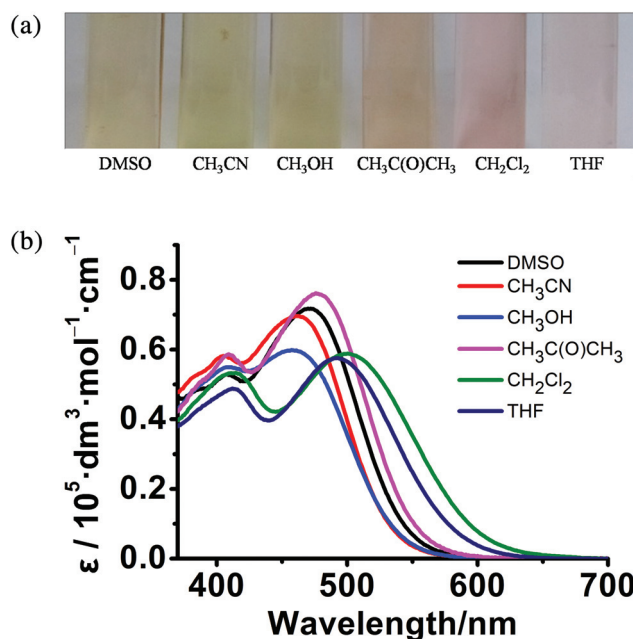**Fig. 4** (a) Colours of **3a** (concentration = 2.7 × 10^{-5} mol dm^{-3}) in various solvents. (b) Electronic absorption spectra of **3a** in 370–700 nm in various solvents at 298 K.

to come from the mixture of ^{3}MLCT (dπ(Pt) → π*(^{t}Bu$_3$tpy)) and ^{3}LLCT (π(acetylide ligand) → π*(^{t}Bu$_3$tpy)) excited states. However, in solutions, complexes **3a–3d** show very weak or no emission at 298 K.

Anion binding properties of complexes 3a–3d in CH$_3$CN

The binding properties of **3a–3d** in CH$_3$CN towards anions, such as F$^-$, Cl$^-$, Br$^-$, I$^-$, OAc$^-$, NO$_3^-$, HSO$_4^-$, SO$_4^{2-}$, and
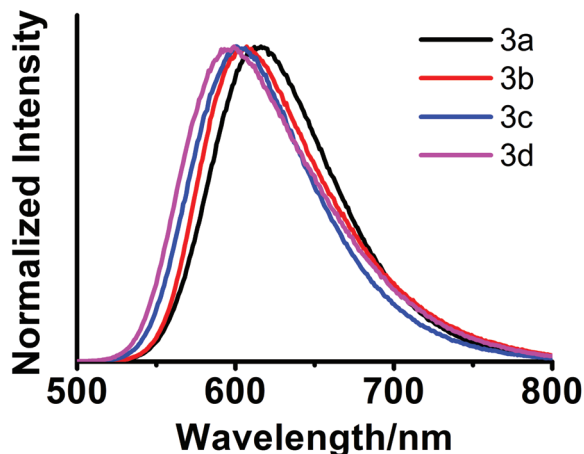
Fig. 5 Emission spectra of **3a–3d** in the solid state at 298 K.

459 nm gradually decreases, while the new absorption bands at 371 and 480 nm appear with the progressively increasing intensity. Consequently, the colour of the solution (5×10^{-5} mol dm^{-3}) changes from pale yellow to light red. Well-defined isosbestic points are observed at 287, 301 and 358 nm, indicating that only two species coexist during the titration equilibrium and suggesting the possible formation of anion-complex adduct. The addition of other anions (Cl$^-$, Br$^-$, I$^-$, OAc$^-$, NO$_3^-$, and HSO$_4^-$) into the CH$_3$CN solution of **3d** causes similar (but smaller) spectral changes to those towards F$^-$ (Fig. S7–S12, ESI†).

For non-nitro-derivatives **3a–3c**, their UV-vis spectral changes in CH$_3$CN are similar to each other upon the addition of anions studied in this study (Fig. S13–S32, ESI†). Fig. 7 demonstrates the UV-vis spectral changes of **3a** upon the addition of F$^-$ in CH$_3$CN at 298 K. During the process, the absorption bands at 405 and 464 nm gradually decrease, and a new band at 485 nm appears. A well-defined isosbestic point is observed at 473 nm. To determine the binding ratio between the complex and anion, the Job's plots have been made. Fig. S33(a) (ESI†) shows the Job's plots of complexes **3a–3d** with F$^-$ in CH$_3$CN. The absorbance maximum appears at *ca.* 0.5, indicating the 1 : 1 complex-anion formation. Using the 1 : 1 binding model and non-linear least-squares fitting, the log K values of **3a–3d** towards different anions were determined (Table 3). For complexes **3a–3d** with the same anion,

H$_2$PO$_4^-$ (used their tetra-*n*-butylammonium salts), have been investigated by the UV-vis titration experiments. Because the precipitates were produced during the titration of **3a–3d** with SO$_4^{2-}$ and H$_2$PO$_4^-$, corresponding investigations were not carried out. Fig. 6 shows the UV-vis spectral changes of **3d** upon the addition of F$^-$ in CH$_3$CN at 298 K. The absorbance of the absorption bands of **3d** at 246, 273, 284, 312, 328, 339 and
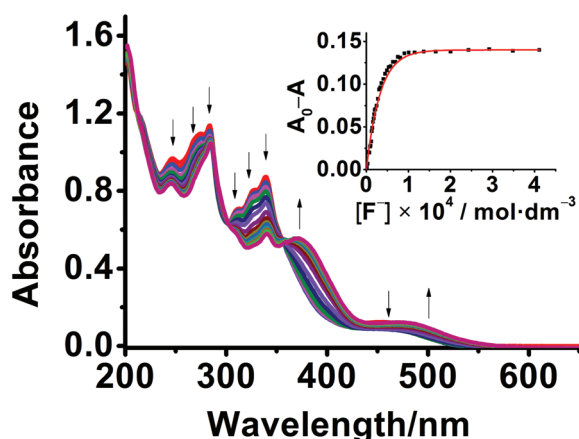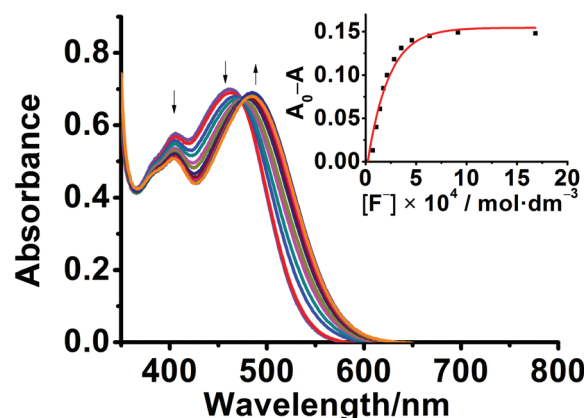

Fig. 6 UV-vis spectral changes of **3d** (5×10^{-5} mol dm^{-3}) in CH$_3$CN upon addition of F$^-$. Inset: A plot of the absorbance change at 250 nm as a function of the concentration of F$^-$ and its theoretical fit for the 1 : 1 binding of complex **3d** with F$^-$.

Fig. 7 UV-vis spectral changes of **3a** (1.2×10^{-4} mol dm^{-3}) in CH$_3$CN upon the addition of F$^-$. Inset: a plot of the absorbance change at 430 nm as a function of the concentration of F$^-$ and its theoretical fit for the 1 : 1 binding of complex **3a** with F$^-$.

Table 3 Binding constants (log K) of **3a–3d** with anions in CH$_3$CN[a]

Complex	F$^-$	OAc$^-$	Cl$^-$	Br$^-$	I$^-$	NO$_3^-$	HSO$_4^-$
3a	4.52 ± 0.14	4.34 ± 0.16	3.35 ± 0.02	2.53 ± 0.03	[b]	2.31 ± 0.06	2.63 ± 0.08
3b	4.88 ± 0.18	4.48 ± 0.21	3.51 ± 0.03	2.75 ± 0.07	2.34 ± 0.15	2.82 ± 0.13	2.92 ± 0.05
3c	5.07 ± 0.51	4.96 ± 0.13	3.80 ± 0.06	2.92 ± 0.05	2.48 ± 0.06	2.90 ± 0.14	3.02 ± 0.13
3d	5.53 ± 0.11	5.22 ± 0.21	3.85 ± 0.08	3.03 ± 0.04	2.60 ± 0.05	2.91 ± 0.09	3.09 ± 0.05

[a] Binding constants were determined by 1 : 1 model using nonlinear fitting methods. [b] Spectral changes were not suitable for accurate measurement of the binding constant.

their log K values are in the following order: R = NO$_2$ (**3d**) > CF$_3$ (**3c**) > Cl (**3b**) > H (**3a**), which is in accordance with the decreasing electron-withdrawing ability of the substituent R on the acetylide ligand of **3a–3d**. This result could be rationalized by the fact that the electron-withdrawing substituent R on the acetylide ligand of **3a–3d** would increase the acidity of urea N–H(s) and strengthen the hydrogen bond interactions between the urea N–H(s) of the complexes and anions. In addition, for the same complex with different anions, the log K values are in the following order: F$^-$ > OAc$^-$ > Cl$^-$ > Br$^-$ ≈ HSO$_4^-$ ≈ NO$_3^-$ > I$^-$, which is in accordance with the decrease in the basicity of the anions.

Anion binding abilities of complexes of 3a–3d towards F$^-$ in DMSO

In our previous study on the anion sensing studies of gold(I) acetylide complexes,[13b] the deprotonation process of the N–H of urea group could be observed upon the addition of F$^-$ into the DMSO solution of gold(I) acetylide complex with the nitro-group. To examine this phenomenon in the platinum(II) complex **3d**, the UV-vis and ^{1}H NMR titration experiments of **3d** towards F$^-$ in DMSO and DMSO-d_6 have been performed. Fig. 8(a) and (b) show the UV-vis spectral changes of **3d** in DMSO upon the addition of F$^-$ at 298 K. When 0–9 equivalents of F$^-$ are added, the absorbance of the absorption bands at 285, 332, as well as 346 nm gradually decreases, while the absorbance at 379 and 489 nm increases. Well-defined isosbestic points are observed at 308 and 371 nm (Fig. 8(a)). After more than 9 equivalents of F$^-$ are added, well-defined isosbestic points are observed at 296, 326 and 420 nm, and the absorbance intensity of the band at 489 nm increases remarkably (Fig. 8(b)). Thus, the colour of the solution of **3d** gradually changes from yellow to red. We propose that two processes occur upon the addition of F$^-$ into the DMSO solution of **3d**. The first one is the hydrogen bond interaction between the urea N–H(s) of **3d** and F$^-$, which occurs at low concentrations of F$^-$. The second one is the deprotonation of the urea N–H of **3d** when the concentration of F$^-$ is high. The appearance of the low-energy absorption band at 489 nm is ascribed to the deprotonation of the urea N–H of **3d** (*vide infra*). In contrast, upon the stepwise addition of F$^-$ into **3a–3c** in DMSO (Fig. S34–S36, ESI†), the colour changes from yellow to orange and UV-vis spectral changes are similar to those of **3a–3c** with F$^-$ in CH$_3$CN (Fig. S13, S19 and S26, ESI†, respectively). The binding constants of **3a–3c** with F$^-$ in DMSO are smaller than those in CH$_3$CN (Table S5, ESI†). This result could be rationalized by the fact that the DMSO solvent could compete with F$^-$ to form hydrogen bonds with urea group of **3a–3c** and reduce the binding abilities of **3a–3c** towards F$^-$. The UV-vis spectral changes of **3d** towards OAc$^-$ in DMSO (Fig. S37, ESI†) are different from those of **3d** towards F$^-$ and are similar to those of **3d** towards OAc$^-$ in CH$_3$CN; furthermore, the colour of the solution changes from yellow to orange. Moreover, the addition of other anions (Cl$^-$, Br$^-$, NO$_3^-$, and HSO$_4^-$) into the DMSO solution of **3d** causes a slight spectral change (Fig. S38–S41, ESI†, respectively). For **3a–3c**, the addition of OAc$^-$ can
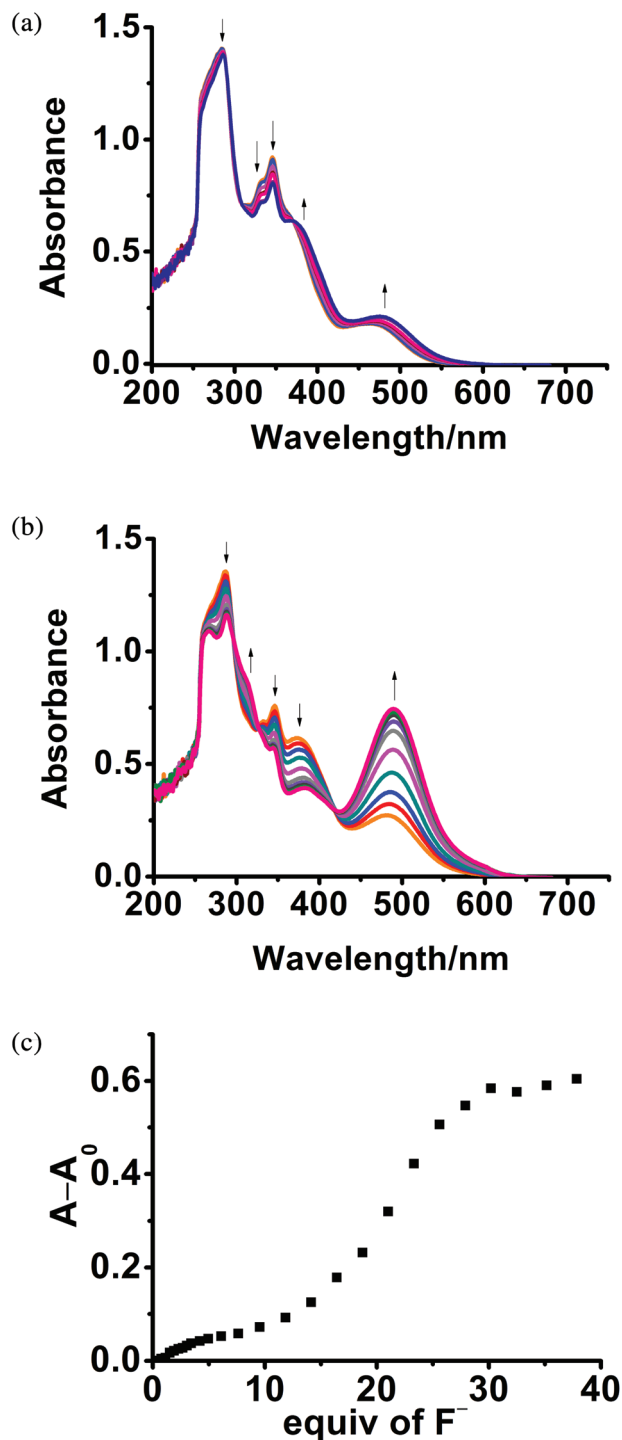
Fig. 8 UV-vis spectral changes of **3d** (3×10^{-5} mol dm^{-3}) in DMSO upon the addition of F$^-$: (a) 0–9 equiv., (b) 9–13 equiv.; (c) a plot of the absorbance change at 489 nm as a function of the concentration of F$^-$.

cause a slight spectral change but the addition of Cl$^-$, Br$^-$, NO$_3^-$, and HSO$_4^-$ also produces a slight spectral change in DMSO solution (Fig. S42–S55, ESI†).

The ^{1}H NMR titrations experiments of **3d** with F$^-$ and OAc$^-$ have also been carried out. Fig. 9 shows the spectral changes

Fig. 9 ^{1}H NMR spectral changes of **3d** upon the addition of OAc$^-$ in DMSO-d_6.

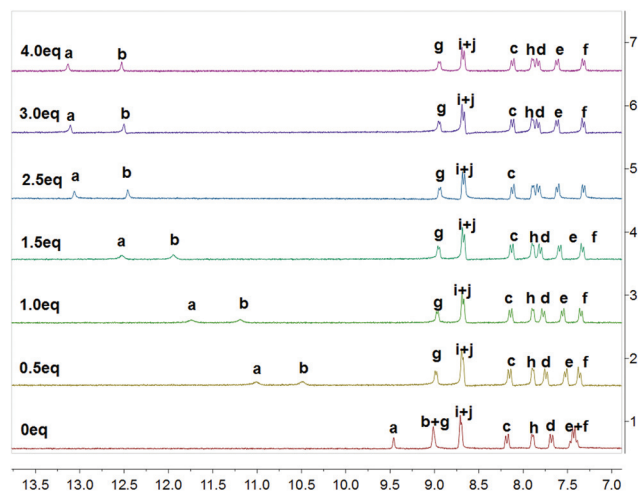of **3d** upon the addition of OAc$^-$ in DMSO-d_6. An obvious downfield shift of urea N–H (H$_a$ and H$_b$) is found upon the addition of OAc$^-$ from 0 to 2.5 equiv. Further addition after 3.0 equiv. does not cause any spectral changes. This result indicates that there are hydrogen bond interactions between the urea N–Hs of **3d** and the acetate anion. The signals of H$_{c-g}$ undergo a slight upfield or downfield shift upon the addition of OAc$^-$ from 0 to 4.0 equiv., which may be due to the through-bond propagation or through-space effect, respectively.[30] Fig. 10 shows the ^{1}H NMR spectral changes of **3d** upon the addition of F$^-$ in DMSO-d_6. Upon the addition of 0.2 equiv. of F$^-$ into the DMSO-d_6 solution of **3d**, the signals of the urea
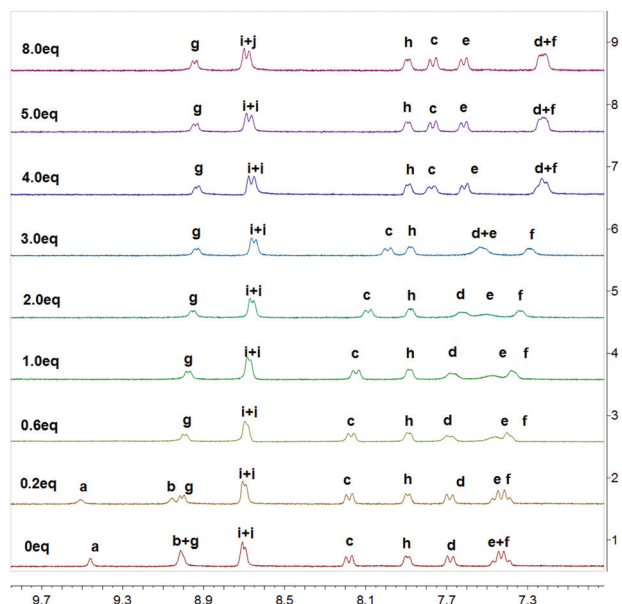
protons (H$_a$ and H$_b$) disappear and the signals of H$_{c-f}$ show a slight shift. After 4 equiv. of F$^-$ is added, a triplet centred at 16.10 ppm (J = 120 Hz), which is assigned as the signal of HF$_2^-$, appears (Fig. S56, ESI†). The signals of H$_{c-f}$ on the acetylide ligand exhibits a slight shift when the amount of F$^-$ added is less than 2 equiv. Upon the addition of more than 2 equiv. of F$^-$, H$_c$, H$_d$, and H$_f$ show the dramatic upfield shift, which could be due to the enhancement of shielding effect, resulting from the increased electron density of aromatic ring through the increased through-bond negative charge delocalization that is caused by the deprotonation process of urea N–H on the acetylide ligand.[30d] In ^{19}F NMR spectra, when the addition of F$^-$ into the DMSO-d_6 solution of **3d** is larger than 3 equiv., a doublet centred at −142.5 ppm (J = 129 Hz) is observed, suggesting the formation of HF$_2^-$ (Fig. S57, ESI†). This result also supports the deprotonation process of the urea N–H of **3d** in DMSO-d_6.

Conclusion

Platinum(II) acetylide complexes bearing urea group **3a–3d** have been synthesized and characterized. These complexes show orange light emission in the solid state at 298 K, which comes from the ^{3}MLCT/^{3}LLCT excited states. In CH$_3$CN, the anion-binding constant (log K) of this class of complexes towards the same anion depends on the substituent R on the acetylide ligand of **3a–3d**: R = NO$_2$ (**3d**) > CF$_3$ (**3c**) > Cl (**3b**) > H (**3a**). In addition, for the same complex with different anions, the log K values follow this order: F$^-$ > OAc$^-$ > Cl$^-$ > Br$^-$ ≈ HSO$_4^-$ ≈ NO$_3^-$ > I$^-$. In DMSO, **3d** shows the selective colour change towards F$^-$, and this is ascribed to the deprotonation of urea N–H of the acetylide ligand of **3d**. The solvent-dependent and selective colour change of **3d** towards F$^-$ allows the naked eye detection of F$^-$.

Experimental

Materials and reagents

[Pt(^{t}Bu$_3$tpy)Cl](OTf) (**2**) was synthesized according to the literature procedure.[31] 4-Ethynylaniline was obtained from Acros. 4-Chlorophenyl isocyanate, K$_2$PtCl$_4$, LiClO$_4$ and LiSO$_3$CF$_3$ were obtained from Energy Chemical. 4-Trifluoromethyl isocyanate, and 4-nitrophenyl isocyanate were obtained from J&K. 4,4′,4″-Tri-*tert*-butyl-2,2′:6′,2″-terpyridine was obtained from Sigma-Aldrich. The solvents were dried and distilled, prior to use except that those used for spectroscopic measurements were of spectroscopic grade. Other reagents were purchased from commercial sources and used as received unless stated otherwise. All the reactions were carried out under anhydrous and anaerobic conditions using standard Schlenk techniques under nitrogen.

Synthesis

HC≡CC$_6$H$_4$-4-NHC(O)NHC$_6$H$_5$ (1a). A mixture of 4-ethynyl-aniline (300 mg, 2.56 mmol) and isocyanatobenzene (391 mg,

Fig. 10 ^{1}H NMR spectral changes of **3d** upon the addition of F$^-$ in DMSO-d_6 at 6.90−9.85 ppm.

2.54 mmol) in dichloromethane (30 mL) was refluxed for 24 h under N_2. The yellow precipitate was collected and washed with dichloromethane and diethyl ether. Yield: 555 mg, 80%. ^{1}H NMR (300 MHz, DMSO-d_6, 298 K) δ = 8.85 (s, 1H, NH), 8.70 (s, 1H, NH), 7.43 (t, J = 7.0 Hz, 4H, aromatic ring), 7.76–7.35 (m, 6H, aromatic ring), 7.26 (t, J = 8 Hz, 2H, aromatic ring), 6.96 (s, 1H, aromatic ring), 4.03 (s, 1H, HC≡C). IR (KBr, cm^{-1}): ν = 3293 (N–H), 1627 (C=O). Anal. calcd for $C_{15}H_{12}N_2O$: C, 76.25; H, 5.12; N, 11.86%. Found: C, 76.55; H, 5.08; N, 11.67%.

HC≡CC$_6$H$_4$-4-NHC(O)NHC$_6$H$_4$-4-Cl (1b). The procedure was similar to that of complex **1a**, except 4-chlorophenyl isocyanate was used instead of isocyanatobenzene. Yield: 540 mg, 78%. ^{1}H NMR (300 MHz, DMSO-d_6, 298 K) δ = 8.90 (s, 1H, NH), 8.86 (s, 1H, NH), 7.47–7.38 (m, 4H, aromatic ring), 7.35–7.29 (m, 4H, aromatic ring), 4.04 (s, 1H, HC≡C). IR (KBr, cm^{-1}): ν = 3281 (N–H), 1641 (C=O). Anal. calcd for $C_{15}H_{11}ClN_2O$: C, 66.55; H, 4.10; N, 13.09%. Found: C, 66.38; H, 4.12; N, 13.01%.

HC≡CC$_6$H$_4$-4-NHC(O)NHC$_6$H$_4$-4-CF$_3$ (1c). The procedure was similar to that of complex **1a**, except 4-trifluoromethyl isocyanate was used instead of isocyanatobenzene. Yield: 466 mg, 72%. ^{1}H NMR (300 MHz, DMSO-d_6, 298 K) δ = 9.14 (s, 1H, NH), 9.00 (s, 1H, NH), 7.62 (s, 4H, aromatic ring), 7.46 (d, J = 9 Hz, 2H, aromatic ring), 7.38 (d, J = 9 Hz, 2H, aromatic ring), 4.05 (s, 1H, HC≡C). IR (KBr, cm^{-1}): ν = 3321 (N–H), 1647 (C=O). Anal. calcd for $C_{16}H_{11}F_3N_2O$: C, 63.16; H, 3.64; N, 9.21%. Found: C, 62.98; H, 3.63; N, 9.11%.

HC≡CC$_6$H$_4$-4-NHC(O)NHC$_6$H$_4$-4-NO$_2$ (1d). The procedure was similar to that of complex **1a**, except 4-nitrophenyl isocyanate was used instead of isocyanatobenzene. Yield: 166 mg, 46%. ^{1}H NMR (300 MHz, DMSO-d_6, 298 K) δ = 9.46 (s, 1H, NH), 9.10 (s, 1H, NH), 8.18 (d, J = 9 Hz, 2H, aromatic ring), 7.67 (d, J = 9 Hz, 2H, aromatic ring), 7.48 (d, J = 9 Hz, 2H, aromatic ring), 7.40 (d, J = 8.6 Hz, 2H, aromatic ring), 4.06 (s, 1H, HC≡C). IR (KBr, cm^{-1}): ν = 3290 (N–H), 1641 (C=O). Anal. calcd for $C_{15}H_{11}N_3O_3$: C, 64.05; H, 3.94; N, 14.94%. Found: C, 63.98; H, 3.93; N, 14.94%.

[Pt(^{t}Bu$_3$tpy)(C≡CC$_6$H$_4$-4-NHC(O)NHC$_6$H$_5$)](OTf) (3a). A mixture of **2** (70 mg, 0.088 mmol), **1a** (24 mg, 0.089 mmol), CuI (5 mg, 0.026 mmol), and diisopropylamine (1 mL) in dichloromethane (25 mL) was stirred for 18 h at room temperature. The orange precipitate was collected and washed with diethyl ether. The product was recrystallized from acetonitrile. Yield: 69 mg, 80%. ^{1}H NMR (300 MHz, DMSO-d_6, 298 K) δ = 8.89 (d, J = 7 Hz, 2H, tpy), 8.74 (s, 1H, NH), 8.66–8.65 (m, 5H, tpy + NH), 7.85 (dd, J = 6 Hz, 2 Hz, 2H, tpy), 7.48–7.40 (m, 4H, aromatic ring), 7.42–7.35 (m, 2H, aromatic ring), 7.27 (t, J = 8 Hz, 2H, aromatic ring), 6.96 (t, J = 8 Hz, 1H, aromatic ring), 1.52 (s, 9H, ^{t}Bu), 1.43 (s, 18H, ^{t}Bu). IR (KBr, cm^{-1}): ν = 3420 (N–H), 1612 (C=O). ESI-MS: m/z = 832 [M − OTf]$^+$. Anal. calcd for $C_{43}H_{46}F_3N_5O_4PtS$: C, 52.65; H, 4.75; N, 7.14%. Found: C, 52.61; H, 4.76; N, 7.13%.

[Pt(^{t}Bu$_3$tpy)(C≡CC$_6$H$_4$-4-NHC(O)NHC$_6$H$_4$-4-Cl)](OTf) (3b). The procedure was similar to that of complex **3a**, except **1b** was used instead of **1a**. Yield: 45 mg, 59%. ^{1}H NMR (300 MHz, DMSO-d_6, 298 K) δ = 9.02 (d, J = 7 Hz, 2H, tpy), 8.85 (s, 1H, NH), 8.81 (s, 1H, NH), 8.71–8.70 (m, 4H, tpy), 7.90 (dd, J = 6 Hz, 2 Hz, 2H, tpy), 7.49–7.30 (m, 8H, aromatic ring), 1.52 (s, 9H, ^{t}Bu), 1.43 (s, 18H, ^{t}Bu). IR (KBr, cm^{-1}): ν = 3356 (N–H), 1641 (C=O). ESI-MS: m/z = 866 [M − OTf]$^+$. Anal. calcd for $C_{43}H_{45}ClF_3N_5O_4PtS$: C, 50.86; H, 4.47; N, 6.90%. Found: C, 50.87; H, 4.46; N, 6.86%.

[Pt(^{t}Bu$_3$tpy)(C≡CC$_6$H$_4$-4-NHC(O)NHC$_6$H$_4$-4-CF$_3$)](OTf) (3c). The procedure was similar to that of complex **3a**, except **1c** was used instead of **1a**. Yield: 55 mg, 63%. ^{1}H NMR (300 MHz, DMSO-d_6, 298 K) δ = 9.17 (s, 1H, NH), 8.94 (s, br, 3H, tpy + NH), 8.69–8.65 (m, 4H, tpy), 7.87 (dd, J = 6 Hz, 2 Hz, 2H, tpy), 7.66–7.64 (m, 4H, aromatic ring), 7.45 (d, J = 8.9 Hz, 2H, aromatic ring), 7.38 (d, J = 8.6 Hz, 2H, aromatic ring), 1.52 (s, 9H, ^{t}Bu), 1.43 (s, 18H, ^{t}Bu). IR (KBr, cm^{-1}): ν = 3433 (N–H), 1610 (C=O). ESI-MS: m/z = 900 [M − OTf]$^+$. Anal. calcd for $C_{44}H_{45}F_6N_5O_4PtS$: C, 50.38; H, 4.32; N, 6.68%. Found: C, 50.40; H, 4.30; N, 6.67%.

[Pt(^{t}Bu$_3$tpy)(C≡CC$_6$H$_4$-4-NHC(O)NHC$_6$H$_4$-4-NO$_2$)](OTf) (3d). The procedure was similar to that of complex **3a**, except **1d** was used instead of **1a**. Yield: 50 mg, 70%. ^{1}H NMR (300 MHz, DMSO-d_6, 298 K) δ = 9.46 (s, 1H, NH), 9.01 (s, br, 3H, tpy + NH), 8.71–8.69 (m, 4H, tpy), 8.18 (d, J = 9 Hz, 2H, aromatic ring), 7.89 (dd, J = 6 Hz, 2 Hz, 2H, tpy), 7.68 (d, J = 9 Hz, 2H, aromatic ring), 7.47–7.39 (m, 4H, aromatic ring), 1.53 (s, 9H, ^{t}Bu), 1.44 (s, 18H, ^{t}Bu). IR (KBr, cm^{-1}): ν = 3350 (N–H), 2054 (C≡C), 1620 (C=O). ESI-MS: m/z = 877 [M − OTf]$^+$. Anal. calcd for $C_{43}H_{45}F_3N_6O_6PtS$: C, 50.34; H, 4.42; N, 8.19%. Found: C, 50.06; H, 4.48; N, 8.27%.

Measurements and instrumentation

Electronic absorption spectra were measured on a PGENERAL TU1901 UV-vis spectrophotometer. Emission spectra were obtained on a FLSP920 fluorescence spectrophotometer. Chemical shifts (δ, ppm) were reported relative to tetramethylsilane for ^{1}H NMR and NaF (δ = −122.4 ppm) for ^{19}F NMR on a Varian Mercury−Plus 300 spectrometer. Infrared spectra were recorded from KBr pellets in the range 400–4000 cm^{-1} on a Bruker-EQUINOX 55 FT-IR spectrometer. Electrospray ionization (ESI) mass spectra were recorded on a LCQ DECA XP quadrupole ion trap mass spectrometer. Elemental analysis was performed on an Elementar Vario EL elemental analyzer.

Crystal structure determination

Crystals of **3a**, **3b·CH$_3$CN**, and **3c·CH$_3$CN** were grown by the diffusion of diethyl ether into DMF–MeOH (v/v = 1), DMF–CH$_3$CN (v/v = 1), and DMF–CH$_3$CN (v/v = 1) solutions, respectively. Crystals of **3a·DMF·THF** were obtained by layering diethyl ether onto DMF–THF (v/v = 1) solution. Selected single crystals of **3b·CH$_3$CN** and **3c·CH$_3$CN** were used for data collection on a Rigaku R-AXIS Spider IP with graphite monochromatized Mo-Kα radiation (λ = 0.71073 Å) and Cu-Kα (λ = 1.54178 Å), respectively, while **3a** and **3a·DMF·THF** were obtained by Oxford Gemini S Ultra CCD area detector diffractometer with graphite monochromatized Mo-Kα radiation (λ = 0.71073 Å). An empirical absorption correction was applied using the PROCESS-AUTO (Rigaku, 1998) or CrysAlisPro (Version

1.171.36.32) program. The structures were solved by direct methods and refined by the full-matrix least-square method based on F^2 with the program SHELXL-2013 using the OLEX2 software package.[32] In **3a**, large regions of diffuse electron density that could not be modeled (disordered solvents) were removed from the refinement, using SQUEEZE function in PLATON (see cif for details). CCDC 1028565, 1028514, 1028592, and 1028516 contain the supplementary crystallographic data for **3a**, **3a·DMF·THF**, **3b·CH₃CN**, and **3c·CH₃CN**, respectively.

Titrations and Job's plot

For a typical UV-vis titration experiment of **3a–3d** in CH₃CN, 0.2 μL aliquots of a tetra-*n*-butylammonium salt (concentrations from 2.0×10^{-3} mol dm^{-3} to 5.0×10^{-3} mol dm^{-3}) were added into the 3 mL solution of the complex (**3a–3c**: from 1.2×10^{-4} mol dm^{-3} to 2.5×10^{-4} mol dm^{-3}; **3d**: 5×10^{-4} mol dm^{-3}) by a syringe, and the spectral changes were recorded by a PGENERAL TU1901 UV-vis spectrophotometer at 298 K. The UV-vis titration experiments in DMSO were the same as those in CH₃CN, expect the concentration of **3a–3d** was changed to 3×10^{-4} mol dm^{-3}. For a typical ^{1}H NMR titration experiment of **3d** in DMSO-d_6, 0.5 μL aliquots of a tetra-*n*-butylammonium salt ([F$^-$] = 0.25 mol dm^{-3}, [OAc$^-$] = 0.3 mol dm^{-3} in DMSO-d_6) were gradually added into the 0.5 mL solution of the complex 3d in DMSO-d_6 (9.7×10^{-4} mol dm^{-3}) by a syringe, and the ^{1}H NMR and ^{19}F NMR spectral changes were recorded by a Varian Mercury-Plus 300 spectrometer at 298 K. The binding constant $\log K$ values were determined by nonlinear fitting using 1:1 model.[33] Job's plots were obtained from a series of solutions in which the fraction of the corresponding anions varied, keeping the total concentration (the complexes and anions) constant. The maxima of the plots indicated the binding stoichiometry of the complexes with anions.

Acknowledgements

Notes and references

1 (a) P. A. Gale, N. Busschaert, C. J. E. Haynes, L. E. Karagiannidis and I. L. Kirby, *Chem. Soc. Rev.*, 2014, **43**, 205–241; (b) F. Wang, L. Wang, X. Chen and J. Yoon, *J. Chem. Soc. Rev.*, 2014, **43**, 4312–4324; (c) L. Fabbrizzi and A. Poggi, *Chem. Soc. Rev.*, 2013, **42**, 1681–1699; (d) P. A. Gale, *Acc. Chem. Res.*, 2011, **44**, 216–226; (e) Z. Xu, X. Chen, H. N. Kim and J. Yoon, *Chem. Soc. Rev.*, 2010, **39**, 127–137; (f) S. Kubik, *Chem. Soc. Rev.*, 2010, **39**, 3648–3663; (g) C. Caltagirone and P. A. Gale, *Chem. Soc. Rev.*, 2009, **38**,

520; (h) A. P. Davis, *Coord. Chem. Rev.*, 2006, **250**, 2939–2951.

2 C. H. Park and H. E. Simmons, *J. Am. Chem. Soc.*, 1968, **90**, 2431–2431.

3 (a) N. H. Evans and P. D. Beer, *Angew. Chem., Int. Ed.*, 2014, **53**, 11716–11754; (b) Z. Guo, I. Shin and J. Yoon, *Chem. Commun.*, 2012, **48**, 5956–5967; (c) H. T. Ngo, X. Liu and K. A. Jolliffe, *Chem. Soc. Rev.*, 2012, **41**, 4928–4925; (d) R. M. Duke, E. B. Veale, F. M. Pfeffer, P. E. Kruger and T. Gunnlaugsson, *Chem. Soc. Rev.*, 2010, **39**, 3936–3953; (e) J. W. Steed, *Chem. Soc. Rev.*, 2009, **38**, 506–519.

4 (a) V. Amendola, G. Bergamaschi, M. Boiocchi, L. Fabbrizzi and L. Mosca, *J. Am. Chem. Soc.*, 2013, **135**, 6345–6355; (b) L. Fabbrizzi, V. Amendola and L. Mosca, *Chem. Soc. Rev.*, 2010, **39**, 3889–3915.

5 A. F. Li, J. H. Wang, F. Wang and Y. B. Jiang, *Chem. Soc. Rev.*, 2010, **39**, 3729–3745.

6 (a) M. A. Hossain, R. A. Begum, V. W. Day and K. Bowman-James, *Amide and urea-based receptors. Supramolecular Chemistry: From Molecules to Nanomaterials*, Wiley, Hoboken, NJ, 2012, vol 3, 1153–1178; (b) C. R. Bondy and S. J. Loeb, *Coord. Chem. Rev.*, 2003, **240**, 77–99.

7 M. D. Best, S. L. Tobey and E. V. Anslyn, *Coord. Chem. Rev.*, 2003, **240**, 3–15.

8 (a) P. A. Gale and C. Caltagirone, *Chem. Soc. Rev.*, 2015, DOI: 10.1039/c4cs00179f; (b) E. B. Veale and T. Gunnlaugsson, *Annu. Rep. Prog. Chem., Sect. B*, 2010, **106**, 376–406.

9 (a) N. H. Evans, C. J. Serpell, K. E. Christensen and P. D. Beer, *Eur. J. Inorg. Chem.*, 2012, 939–944; (b) D. P. Cormode, A. J. Evans, J. J. Davis and P. D. Beer, *Dalton Trans.*, 2010, **39**, 6532–6541; (c) Y. Willener, K. M. Joly, C. J. Moody and J. H. R. Tucker, *J. Org. Chem.*, 2008, **73**, 1225–1233; (d) F. Oton, A. Tarraga, A. Espinosa, M. D. Velasco and P. Molina, *J. Org. Chem.*, 2006, **71**, 4590–4598; (e) F. Oton, A. Tarraga, M. D. Velasco and P. Molina, *Dalton Trans.*, 2006, 3685–3692; (f) F. Oton, A. Tarraga, M. D. Velasco and P. Molina, *Dalton Trans.*, 2005, 1159–1161; (g) P. D. Beer and S. R. Bayly, *Top. Curr. Chem.*, 2005, **255**, 125–162; (h) F. Oton, A. Tarraga, M. D. Velasco, A. Espinosa and P. Molina, *Chem. Commun.*, 2004, 1658–1659; (i) H. Miyaji, S. R. Collinson, I. Prokes and J. H. R. Tucker, *Chem. Commun.*, 2003, 64–65; (j) A. J. Evans, S. E. Matthews, A. R. Cowley and P. D. Beer, *Dalton Trans.*, 2003, 4644–4650; (k) B. Alonso, C. M. Casado, I. Cuadrado, M. Moran and A. E. Kaifer, *Chem. Commun.*, 2002, 1778–1779; (l) P. D. Beer, J. Cadam, J. M. Loris, R. Martinez-Manez, M. E. Padilla, T. Pardo, D. K. Smith and J. Soto, *Dalton Trans.*, 1999, 127–134.

10 (a) A. Ramdass, V. Sathish, M. Velayudham, P. Thanasekaran, K. L. Lu and S. Rajagopal, *Inorg. Chem. Commun.*, 2013, **35**, 186–191; (b) M. O. Odago, A. E. Hoffman, R. L. Carpenter, D. C. T. Tse, S. S. Sun and A. J. Lees, *Inorg. Chim. Acta*, 2011, **374**, 558–565.

11 (a) G. Baggi, M. Boiocchi, C. Ciarrocchi and L. Fabbrizzi, *Inorg. Chem.*, 2013, **52**, 5273–5283; (b) Y. J. P. Hao, J. Yang,

S. G. Li, X. J. Huang, X. J. Yang and B. Wu, *Dalton Trans.*, 2012, **41**, 7689–7694; (*c*) A. Ghosh, S. Verma, B. Ganguly, H. N. Ghosh and A. Das, *Eur. J. Inorg. Chem.*, 2009, **2009**, 2496–2507; (*d*) A. Ghosh, B. Ganguly and A. Das, *Inorg. Chem.*, 2007, **46**, 9912–9918.

12 Y. Li, Y. Liu, D. Nam, S. Park, J. Yoon and M. H. Hyun, *Dyes Pigm.*, 2014, **100**, 241–246.

13 (*a*) C. L. Li, Q. R. Guan, X. C. Li, J. Wang, Y. P. Zhou, D. G. Churchill and H. Y. Chao, *Inorg. Chem. Commun.*, 2013, **35**, 149–151; (*b*) Y. P. Zhou, M. Zhang, Y. H. Li, Q. R. Guan, F. Wang, Z. J. Lin, C. K. Lam, X. L. Feng and H. Y. Chao, *Inorg. Chem.*, 2012, **51**, 5099–5109; (*c*) X. He, F. Herranz, E. C. C. Cheng, R. Vilar and V. W. W. Yam, *Chem. – Eur. J.*, 2010, **16**, 9123–9131; (*d*) X. He and V. W. W. Yam, *Inorg. Chem.*, 2010, **49**, 2273–2279.

14 (*a*) C. M. G. dos Santos and T. Gunnlaugsson, *Dalton Trans.*, 2009, **24**, 4712–4721; (*b*) C. M. G. dos Santos, P. B. Fernandez, S. E. Plush, J. P. Leonard and T. Gunnlaugsson, *Chem. Commun.*, 2007, 3389–3391.

15 X. He, N. Zhu and V. W. W. Yam, *Dalton Trans.*, 2011, **40**, 9703–9710.

16 (*a*) C. L. Ho and W. Y. Wong, *Coord. Chem. Rev.*, 2013, **257**, 1614–1649; (*b*) W. Y. Wong and P. D. Harvey, *Macromol. Rapid Commun.*, 2010, **31**, 671–713; (*c*) W. Y. Wong, *Dalton Trans.*, 2007, 4495–4510; (*d*) W. Y. Wong and C. L. Ho, *Coord. Chem. Rev.*, 2006, **250**, 2627–2690.

17 (*a*) J. Ni, Y. G. Wang, J. Y. Wang, Y. Q. Zhao, Y. Z. Pan, H. H. Wang, X. Zhang, J. J. Zhang and Z. N. Chen, *Dalton Trans.*, 2013, **42**, 13092–13100; (*b*) X. Zhang, B. Li, Z. H. Chen and Z. N. Chen, *J. Mater. Chem.*, 2012, **22**, 11427–11441; (*c*) J. Ni, X. Zhang, N. Qiu, Y. H. Wu, L. Y. Zhang, J. Zhang and Z. N. Chen, *Inorg. Chem.*, 2011, **50**, 9090–9096; (*d*) Z. M. Hudson, C. Sun, K. J. Harris, B. E. G. Lucier, R. W. Schurko and S. Wang, *Inorg. Chem.*, 2011, **50**, 3447–3457; (*e*) J. Ni, Y. H. Wu, X. Zhang, B. Li, L. Y. Zhang and Z. N. Chen, *Inorg. Chem.*, 2009, **48**, 10202–10210; (*f*) J. Ni, L. Y. Zhang, H. M. Wen and Z. N. Chen, *Chem. Commun.*, 2009, 3801–3803; (*g*) M. L. Muro, C. A. Daws and F. N. Castellano, *Chem. Commun.*, 2008, 6134–6136; (*h*) S. C. F. Kui, S. S. Y. Chui, C. M. Che and N. Zhu, *J. Am. Chem. Soc.*, 2006, **128**, 8297–8309; (*i*) W. Lu, M. C. W. Chan, N. Zhu, C. M. Che, Z. He and K. Y. Wong, *Chem. – Eur. J.*, 2003, **9**, 6155–6166; (*j*) V. W. W. Yam, K. M. C. Wong and N. Zhu, *J. Am. Chem. Soc.*, 2002, **124**, 6506–6507.

18 (*a*) C. Y. S. Chung and V. W. W. Yam, *Chem. – Eur. J.*, 2013, **19**, 13182–13192; (*b*) X. Han, L. Z. Wu, G. Si, J. Pan, Q. Z. Yang, L. P. Zhang and C. H. Tung, *Chem. – Eur. J.*, 2007, **13**, 1231–1239; (*c*) K. M. C. Wong, W. S. Tang, X. X. Lu, N. Y. Zhu and V. W. W. Yam, *Inorg. Chem.*, 2005, **44**, 1492–1498.

19 (*a*) V. Uahengo, N. Zhou, B. Xiong, P. Cai, K. Hu and G. Cheng, *J. Organomet. Chem.*, 2013, **732**, 102–108; (*b*) K. M. C. Wong and V. W. W. Yam, *Coord. Chem. Rev.*, 2007, **251**, 2477–2488; (*c*) H. S. Lo, S. K. Yip, K. M. C. Wong, N. Zhu and V. W. W. Yam, *Organometallics*, 2006, **25**, 3537–

3540; (*d*) K. M. C. Wong, W. S. Tang, X. X. Lu, N. Zhu and V. W. W. Yam, *Inorg. Chem.*, 2005, **44**, 1492–1498; (*e*) W. S. Tang, X. X. Lu, K. M. C. Wong and V. W. W. Yam, *J. Mater. Chem.*, 2005, **15**, 2714–2720; (*f*) P. K. M. Siu, S. W. Lai, W. Lu, N. Zhu and C. M. Che, *Eur. J. Inorg. Chem.*, 2003, **15**, 2749–2752; (*g*) V. W. W. Yam, R. P. L. Tang, K. M. C. Wong, C. C. Ko and K. K. Cheung, *Inorg. Chem.*, 2001, **40**, 571–574; (*h*) V. W. W. Yam, R. P. L. Tang, K. M. C. Wong and K. K. Cheung, *Organometallics*, 2001, **20**, 4476–4482; (*i*) A. Diez, E. Lalinde and M. T. Moreno, *Coord. Chem. Rev.*, 2011, **255**, 2426–2447.

20 (*a*) J. Ni, Y. G. Wang, H. H. Wang, L. Xu, Y. Q. Zhao, Y. Z. Pan and J. J. Zhang, *Dalton Trans.*, 2014, **43**, 352–360; (*b*) J. Ni, Y. G. Wang, H. H. Wang, Y. Z. Pan, L. Xu, Y. Q. Zhao, X. Y. Liu and J. J. Zhang, *Eur. J. Inorg. Chem.*, 2014, 986–993.

21 (*a*) A. Han, P. W. Du, Z. J. Sun, H. T. Wu, H. X. Jia, R. Zhang, Z. N. Liang, R. Cao and R. Eisenberg, *Inorg. Chem.*, 2014, **53**, 3338–3344; (*b*) X. Zhang, J. Y. Wang, J. Ni, L. Y. Zhang and Z. N. Chen, *Inorg. Chem.*, 2012, **51**, 5569–5579; (*c*) J. Ni, X. Zhang, Y. H. Wu, L. Y. Zhang and Z. N. Chen, *Chem. – Eur. J.*, 2011, **17**, 1171–1183.

22 (*a*) Y. J. Tian, E. T. Shi, Y. K. Tian, R. S. Yao and F. Wang, *Org. Lett.*, 2014, **16**, 3180–3183; (*b*) Y. Tanaka, K. M. C. Wong and V. W. W. Yam, *Chem. – Eur. J.*, 2013, **19**, 390–399; (*c*) Y. Tanaka, K. M. C. Wong and V. W. W. Yam, *Angew. Chem., Int. Ed.*, 2013, **52**, 14117–14120; (*d*) T. Nabeshima, Y. Hasegawa, R. Trokowski and M. Yamamura, *Tetrahedron Lett.*, 2012, **53**, 6182–6185; (*e*) H. Sun, H. Guo, W. Wu, X. Liu and J. Zhao, *Dalton Trans.*, 2011, **40**, 7834–7841.

23 (*a*) L. Liu, S. Guo, J. Ma, K. Xu, J. Zhao and T. Zhang, *Chem. – Eur. J.*, 2014, **20**, 14282–14295; (*b*) J. J. Zhong, Q. Y. Meng, G. X. Wang, Q. Liu, B. Chen, K. Feng, C. H. Tung and L. Z. Wu, *Chem. – Eur. J.*, 2013, **19**, 6443–6450; (*c*) X. H. Wang, S. Goeb, Z. Q. Ji, N. A. Pogulaichenko and F. N. Castellano, *Inorg. Chem.*, 2011, **50**, 705–707; (*d*) P. Jarosz, P. Du, J. Schneider, S. H. Lee, D. McCamant and R. Eisenberg, *Inorg. Chem.*, 2009, **48**, 9653–9663; (*e*) P. Du, K. Knowles and R. Eisenberg, *J. Am. Chem. Soc.*, 2008, **130**, 12576–12577; (*f*) P. Du, J. Schneider, P. Jarosz and R. Eisenberg, *J. Am. Chem. Soc.*, 2006, **128**, 7726–7727; (*g*) Y. Yang, D. Zhang, L. Z. Wu, B. Chen, L. P. Zhang and C. H. Tung, *J. Org. Chem.*, 2004, **69**, 4788–4791; (*h*) D. Zhang, L. Z. Wu, Q. Z. Yang, X. H. Li, L. P. Zhang and C. H. Tung, *Org. Lett.*, 2003, **5**, 3221–3224.

24 (*a*) E. C. H. Kwok, M. Y. Chan, K. M. C. Wong and V. W. W. Yam, *Chem. – Eur. J.*, 2014, **20**, 3142–3153; (*b*) X. Yi, C. Zhang, S. Guo, J. Ma and J. Zhao, *Dalton Trans.*, 2014, **43**, 1672–1683; (*c*) W. Wu, L. Liu, X. Cui, C. Zhang and J. Zhao, *Dalton Trans.*, 2013, **42**, 14374–14379; (*d*) Q. Liu, H. Zhan, C. L. Ho, F. R. Dai, Y. Y. Fu, Z. Xie, L. Wang, J. H. Li, F. Yan and S. P. Huang, *Chem. – Asian J.*, 2013, **8**, 1892–1900; (*e*) F. R. Dai, H. M. Zhan, Q. Liu, Y. Y. Fu, J. H. Li, Q. W. Wang, Z. Xie, L. Wang, F. Yan and W. Y. Wong, *Chem. – Eur. J.*, 2012, **18**, 1502–1511;

(f) W. Wu, J. Zhao, H. Guo, J. Sun, S. Ji and Z. Wang, *Chem. – Eur. J.*, 2012, **18**, 1961–1968; (g) H. M. Zhan, S. Lamare, A. Ng, T. Kenny, H. Guernon, W. K. Chan, A. B. Djurisic, P. D. Harvey and W. Y. Wong, *Macromolecules*, 2011, **44**, 5155–5167; (h) W. Y. Wong and C. L. Ho, *Acc. Chem. Res.*, 2010, **43**, 1246–1256; (i) E. C. H. Kwok, M. Y. Chan, K. M. C. Wong, W. H. Lam and V. W. W. Yam, *Chem. – Eur. J.*, 2010, **16**, 12244–12254; (j) W. Y. Wong, *Macromol. Chem. Phys.*, 2008, **209**, 14–24; (k) W. Y. Wong, X. Z. Wang, Z. He, A. B. Djurisic, C. T. Yip, K. Y. Cheung, H. Wang, C. S. K. Mak and W. K. Chan, *Nat. Mater.*, 2007, **6**, 521–527; (l) W. Y. Wong, X. Z. Wang, Z. He, K. K. Chan, A. B. Djurisic, K. Y. Cheung, C. T. Yip, A. M. C. Ng, Y. Y. Xi and C. S. K. Mak, *J. Am. Chem. Soc.*, 2007, **129**, 14372–14380; (m) X. Z. Wang, W. Y. Wong, K. Y. Cheung, M. K. Fung, A. B. Djurisic and W. K. Chan, *Dalton Trans.*, 2008, 5484–5494; (n) S. Chakraborty, T. J. Wadas, H. Hester, C. Flaschenreim, R. Schmehl and R. Eisenberg, *Inorg. Chem.*, 2005, **44**, 6284–6293.

25 (a) Y. Li, D. P. K. Tsang, C. K. M. Chan, K. M. C. Wong, M. Y. Chan and V. W. W. Yam, *Chem. – Eur. J.*, 2014, **20**, 13710–13715; (b) K. M. C. Wong, M. M. Y. Chan and V. W. W. Yam, *Adv. Mater.*, 2014, **26**, 5558–5568; (c) E. S. H. Lam, A. Y. Y. Tam, M. Y. Chan and V. W. W. Yam, *Isr. J. Chem.*, 2014, **54**, 986–992; (d) E. S. H. Lam, D. P. K. Tsang, W. H. Lam, A. Y. Y. Tam, M. Y. Chan, W. T. Wong and V. W. W. Yam, *Chem. – Eur. J.*, 2013, **19**, 6385–6397; (e) L. Ho, C. H. Chui, W. Y. Wong, S. M. Aly, D. Fortin, P. D. Harvey, B. Yao, Z. Xie and L. Wang, *Macromol. Chem. Phys.*, 2009, **210**, 1786–1798; (f) W. Y. Wong, G. J. Zhou, Z. He, K. Y. Cheung, A. M. C. Ng, A. B. Djurisic and W. K. Chan, *Macromol. Chem. Phys.*, 2008, **209**, 1319–1332; (g) S. C. Chan, M. C. W. Chan, Y. Wang, C. M. Che, K. K. Cheung and N. Y. Zhu, *Chem. – Eur. J.*, 2001, **7**, 4180–4190.

26 (a) G. J. Zhou and W. Y. Wong, *Chem. Soc. Rev.*, 2011, **40**, 2541–2566; (b) G. J. Zhou, W. Y. Wong, S. Y. Poon, C. Ye and Z. Lin, *Adv. Funct. Mater.*, 2009, **19**, 531–544; (c) T. M. Pritchett, W. F. Sun, F. Q. Guo, B. G. Zhang, M. J. Ferry, J. E. Rogers-Haley, W. Shensky III and A. G. Mott, *Opt. Lett.*, 2008, **33**, 1053–1055; (d) Z. Q. Ji, Y. J. Li and W. F. Sun, *Inorg. Chem.*, 2008, **47**, 7599–7607; (e) G. J. Zhou, W. Y. Wong, C. Ye and Z. Lin, *Adv. Funct. Mater.*, 2007, **17**, 963–975; (f) G. J. Zhou, W. Y. Wong, Z. Lin and C. Ye, *Angew. Chem., Int. Ed.*, 2006, **45**, 6189–6193; (g) G. J. Zhou, W. Y. Wong, D. Cui and C. Ye, *Chem. Mater.*, 2005, **17**, 5209–5217; (h) F. Q. Guo, W. F. Sun, Y. Liu and

K. Schanze, *Inorg. Chem.*, 2005, **44**, 4055–4065; (i) W. F. Sun, Z. X. Wu, Q. Z. Yang, L. Z. Wu and C. H. Tung, *Appl. Phys. Lett.*, 2003, **82**, 850–852.

27 (a) M. C. L. Yeung, B. W. K. Chu and V. V. W. Yam, *ChemistryOpen*, 2014, **3**, 172–176; (b) C. Y. S. Chung and V. W. W. Yam, *Chem. – Eur. J.*, 2014, **20**, 13016–13027; (c) X. X. Lin, Z. H. Li, X. Y. Huang, Y. Jiang, Q. H. Wei and G. N. Chen, *Dalton Trans.*, 2014, **43**, 8861–8867; (d) J. L. Fillaut, H. Akdas-Kilig, E. Dean, C. Latouche and A. Boucekkine, *Inorg. Chem.*, 2013, **52**, 4890–4897; (e) C. Qin, W. Y. Wong and L. Wang, *Macromolecules*, 2011, **44**, 483; (f) S. Shanmugaraju, A. K. Bar, K. W. Chi and P. S. Mukherjee, *Organometallics*, 2010, **29**, 2971–2980; (g) Y. Fan, Y. M. Zhu, F. R. Dai, L. Y. Zhang and Z. N. Chen, *Dalton Trans.*, 2007, 3885–3892.

28 (a) Y. Cao, M. O. Wolf and B. O. Patrick, *Inorg. Chem.*, 2013, **52**, 5636–5638; (b) G. S. M. Tong, Y. C. Law, S. C. F. Kui, N. Zhu, K. H. Leung, D. L. Phillips and C. M. Che, *Chem. – Eur. J.*, 2010, **16**, 6540–6554; (c) J. Ni, L. Y. Zhang and Z. N. Chen, *J. Organomet. Chem.*, 2009, **694**, 339–345; (d) E. Shikhova, E. O. Danilov, S. Kinayyigit, I. E. Pomestchenko, A. D. Tregubov, F. Camerel, P. Retailleau, R. Ziessel and F. N. Castellano, *Inorg. Chem.*, 2007, **46**, 3038–3048; (e) H. S. Lo, S. K. Yip, K. M. C. Wong, N. Zhu and V. W. W. Yam, *Organometallics*, 2006, **25**, 3537–3540; (f) K. M. C. Wong, W. S. Tang, B. W. K. Chu, N. Zhu and V. W. W. Yam, *Organometallics*, 2004, **23**, 3459–3465; (g) V. W. W. Yam, K. M. C. Wong and N. Zhu, *J. Am. Chem. Soc.*, 2002, **124**, 6506–6507.

29 S. Y. L. Leung, A. Y. Y. Tam, C. H. Tao, H. S. Chow and V. W. W. Yam, *J. Am. Chem. Soc.*, 2012, **134**, 1047–1056.

30 (a) D. E. Gomez, L. Fabbrizzi, M. Licchelli and E. Monzani, *Org. Biomol. Chem.*, 2005, **3**, 1495–1500; (b) D. Esteban-Gomez, L. Fabbrizzi and M. Liechelli, *J. Org. Chem.*, 2005, **70**, 5717–5720; (c) M. Boiocchi, L. Del Boca, D. Esteban-Gomez, L. Fabbrizzi, M. Licchelli and E. Monzani, *Chem. – Eur. J.*, 2005, **11**, 3097–3104; (d) M. Boiocchi, L. Del Boca, D. E. Gomez, L. Fabbrizzi, M. Licchelli and E. Monzani, *J. Am. Chem. Soc.*, 2004, **126**, 16507–16514.

31 S. W. Lai, M. C. W. Chan, K. K. Cheung and C. M. Che, *Inorg. Chem.*, 1999, **38**, 4262–4267.

32 O. V. Dolomanov, L. J. Bourhis, R. J. Gildea, J. A. K. Howard and H. Puschmann, OLEX2: A complete structure solution, refinement and analysis program, *J. Appl. Crystallogr.*, 2009, **42**, 339–341.

33 J. Bourson, J. Pouget and B. Valeur, *J. Phys. Chem.*, 1993, **97**, 4552–4557.